

# CBNetV2: A Composite Backbone Network Architecture for Object Detection

Tingting Liang\*, Xiaojie Chu\*, Yudong Liu\*, Yongtao Wang, Zhi Tang, Wei Chu, Jingdong Chen, Haibing Ling

**Abstract**—Modern top-performing object detectors depend heavily on backbone networks, whose advances bring consistent performance gains through exploring more effective network structures. However, designing or searching for a new backbone and pre-training it on ImageNet may require a large number of computational resources, making it costly to obtain better detection performance. In this paper, we propose a novel backbone network, namely CBNetV2, by constructing compositions of *existing* open-sourced pre-trained backbones. In particular, CBNetV2 architecture groups multiple identical backbones, which are connected through composite connections. We also propose a better training strategy with the Assistant Supervision for CBNet-based detectors. Without additional pre-training, CBNetV2 can be integrated into mainstream detectors, including one-stage and two-stage detectors, as well as anchor-based and anchor-free-based ones, and significantly improve their performance by more than 3.0% AP over the baseline on COCO. Also, experiments provide strong evidence showing that composite backbones are more efficient and resource-friendly than pre-trained wider and deeper networks, including manual-based and NAS-based, as well as CNN-based and Transformer-based ones. Particularly, with single-model and single-scale testing, our HTC Dual-Swin-B achieves 58.6% box AP and 51.1% mask AP on COCO *test-dev*, which is significantly better than the state-of-the-art result (*i.e.*, 57.7% box AP and 50.2% mask AP) achieved by a stronger baseline HTC++ with a larger backbone Swin-L. Code will be released at <https://github.com/VDIGPKU/CBNetV2>.

**Index Terms**—Deep Learning, Object Detection, Backbone Networks, Composite Architectures.



## 1 INTRODUCTION

OBJECT detection is one of the fundamental problems in computer vision, serving a wide range of applications such as autonomous driving, intelligent video surveillance, remote sensing, *etc.* In recent years, great progresses have been made for object detection thanks to the booming development of deep convolutional networks [2], and a few excellent detectors have been proposed, *e.g.*, SSD [3], Faster R-CNN [4], RetinaNet [5], ATSS [6], Mask R-CNN [7], Cascade R-CNN [8], *etc.*

Typically, in a Neural Network (NN)-based detector, a backbone network is used to extract basic features for detecting objects, and usually designed originally for image classification and pre-trained on the ImageNet dataset [9]. Intuitively, the more representative features extracted by the backbone, the better the performance of its host detector. Starting from AlexNet [2], deeper and wider backbones have been exploited by mainstream detectors, such as VGG [10], ResNet [11], DenseNet [12], ResNeXt [13], Res2Net [14]. More recently, Transformer [15] based backbones have been explored as well and demonstrated very promising performance. In general, the advances in large backbone pre-training have demonstrated a trend towards more effective and efficient multi-scale representations in object detection.

Despite the encouraging results achieved by large backbone-

based detectors, a natural question to ask is: can their existing pre-trained weights show better representation in object detection? While we can always design or search for a new backbone, pre-training such backbone on ImageNet requires a large computational resource, which makes it expensive to obtain better detection performance. Alternatively, training a detector from scratch can save the cost of pre-training the backbone network on the ImageNet dataset, but requires even more computing resources and training skills.

In this paper, we propose a simple yet efficient approach to combine existing pre-trained weights into a powerful detection backbone. Unlike most previous methods that focus on modular crafting and require pre-training on ImageNet to strengthen the representation, we improve the existing backbone representation ability without additional pre-training but a novel composition method. As shown in Fig. 1, our solution, named *Composite Backbone Network V2* (CBNetV2), groups multiple identical backbones together. Specifically, the parallel backbones (named assisting backbones and lead backbone) are connected through *composite connections*. From left to right in Fig. 1, the outputs of each stage in an assisting backbone flow to the parallel and lower-level stages of its succeeding backbone. Finally, the features of the lead backbone are fed to the neck and detection head for bounding box regression and classification. Contrary to simple network deepening or widening, CBNetV2 integrates the high- and low-level features of multiple backbone networks and gradually expands the receptive field to more efficiently perform object detection. It is worth noting that *we do not need to pre-train CBNetV2 on ImageNet for a detector*; instead, *we only need to initialize each assembled backbone of CBNetV2 with the existing open-sourced pre-trained weights of a single backbone* (*e.g.*, ResNet [11], ResNeXt [13], Res2Net [14], DetNAS [16], and

- Corresponding author: Yongtao Wang. \* indicates equal contribution.
- T. Liang, X. Chu, Y. Liu, Y. Wang, Z. Tang are with the Wangxuan Institute of Computer Technology, Peking University, Beijing 100080, China. E-mail: {tingtingliang, bahuangliuhe, wyt, tangzhi}@pku.edu.cn, chuxiaojie@stu.pku.edu.cn
- W. Chu, J. Cheng are with Ant Group of Alibaba, China. E-mail: weichu.cw@alibaba-inc.com, jingdongchen.cjd@antfin.com
- H. Ling is with Department of Computer Science, Stony Brook University, USA. E-mail: hling@cs.stonybrook.edu
- A preliminary version of this manuscript was published in [1].

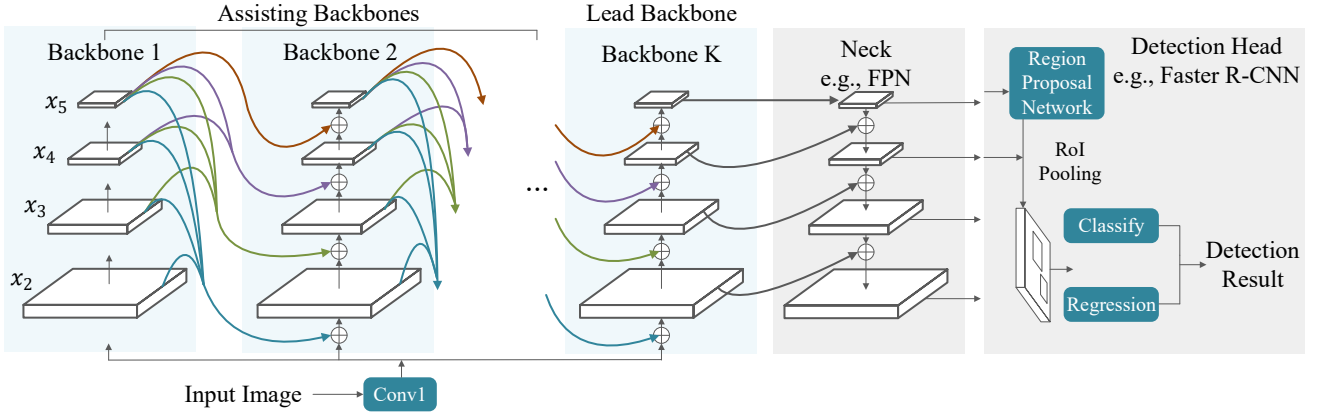


Fig. 1. Illustration of the inference stage of the proposed Composite Backbone Network V2 (CBNetV2) architecture for object detection.

Swin Transformer [17]). In other words, adopting the proposed CBNetV2 is more economical and efficient than designing a new backbone and pre-training it on ImageNet. Further, to further explore the potential of CBNetV2, we propose an effective training strategy with supervision for assisting backbones, achieving higher detection accuracy than the original CBNet [1] without affecting the inference speed.

We demonstrate the effectiveness of our framework by conducting experiments on the challenging MS COCO benchmark [18]. Experiments show that our proposed CBNetV2 enables us to train high-accuracy detectors that significantly outperform the larger backbone-based detectors. We apply CBNetV2 to several mainstream detectors, including one-stage (e.g., RetinaNet [5]) and two-stage (e.g., Faster R-CNN [4], Mask R-CNN [7], Cascade R-CNN and Cascade Mask R-CNN [8]), as well as anchor-based (e.g., Faster R-CNN) and anchor-free-based (e.g., ATSS [6]). The performances of all the above detectors are consistently improved by over 3% AP. Also, the results in Sec. 4 provide strong evidence showing that composite backbones are more efficient than pre-trained wider and deeper networks, including manual-based (e.g., ResNet [11], ResNeXt [13], Res2Net [14]) and NAS-based (e.g., DetNAS [16]), as well as CNN-based (e.g., ResNet) and Transformer-based (e.g., Swin-Transformer [17]). In particular, Dual-ResNeXt50-32x4d<sup>1</sup> is 0.7% AP higher than that of the wider and deeper ResNeXt101-64x4d with only 70% parameter amount; our Dual-Swin-T is 1.7% AP higher than that of the larger Swin-B with fewer FLOPs/Params, advancing the accuracy to 53.6% AP. Specifically, our Cascade R-CNN Dual-Res2Net101 achieves 55.3% AP, and HTC Dual-Swin-B achieves unparalleled single-model single-scale result of 58.6% box AP and 51.1% mask AP on COCO *test-dev*. With multi-scale testing, we push the current best single-model result to a new record of 59.3% box AP and 51.8% mask AP without extra training data.

The main contributions of this paper are listed as follows:

- We originally assemble multiple identical backbones with existing open-sourced pre-trained weights to build a powerful backbone CBNetV2 (Composite Backbone Network V2) for object detection without additional pre-training.
- CBNetV2 uses a more efficient and resource-friendly way to compose large backbones, rather than simply increase

the depth or width of networks and pre-train them on ImageNet.

- Extensive experiments on the COCO benchmark indicate the superiority of our method. Our HTC Dual-Swin-B achieves a new record of single-model single-scale results on COCO. With multi-scale testing, we achieve a single-model-state-of-the-art result without extra training data.

## 2 RELATED WORK

**Object detection.** Object detection aims to locate each object instance from a predefined set of classes from an input image. With the rapid progress of convolutional neural network (CNN), there is a popular paradigm for deep learning-based object detectors: a backbone network (usually designed for classification and pre-trained on ImageNet) extracts basic features from the input image, and then a neck (e.g., a feature pyramid network [20]) enhances the multi-scale features from the backbone, and following that, a detection head outputs the predict boxes with position and classification information. According to the differences of detection heads, the cutting edge methods for general object detection can be briefly categorized into two major branches. The first branch contains one-stage detectors such as YOLO [21], SSD [3], RetinaNet [5], NAS-FPN [22] and EfficientDet [23]. The other branch contains two-stage methods such as Faster R-CNN [4], FPN [20], Mask R-CNN [7], Cascade R-CNN [8] and Libra R-CNN [24]. Recently, academic attention has been geared toward anchor-free detectors due partly to the emergence of FPN [20] and focal Loss [5], more elegant end-to-end detectors have been proposed. On the one hand, FSAF [25], FCOS [26], ATSS [6] and GFL [27] improve RetinaNet with center-based anchor-free methods. On the other hand, CornerNet [28] and CenterNet [29] detect object bounding boxes with a keypoint-based method.

More recently, Neural Architecture Search (NAS) is applied to automatically search the architecture for a specific detector. NAS-FPN [22], NAS-FCOS [30] and SpineNet [31] use reinforcement learning to control the architecture sampling and obtain promising results. SM-NAS [32] uses evolutionary algorithm and partial order pruning method to search the optimal combination of different parts of the detectors. Auto-FPN [33] uses the gradient-based method to search the optimal detector. DetNAS [16] uses the one-shot method to search for an efficient backbone for object detection.

1. Here and after, Dual-Backbone (DB) and Triple-Backbone (TB) respectively represent composing 2 and 3 identical backbones.

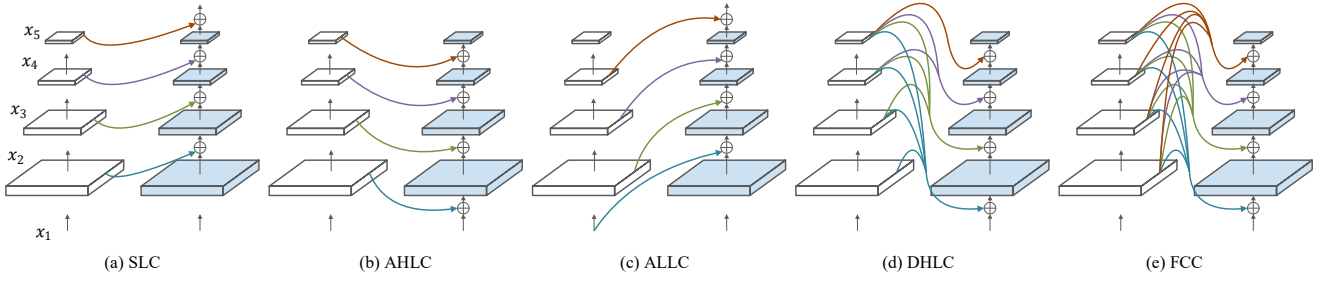


Fig. 2. Four kinds of composite styles for Dual-Backbone architecture (an assisting backbone and a lead backbone). (a) Same Level Composition (SLC). (b) Adjacent Higher-Level Composition (AHLC). (c) Adjacent Lower-Level Composition (ALLC). (d) Dense Higher-Level Composition (DHLC). (e) Full-connected Composition (FCC). The composite connection are colored lines representing some simple operations, *i.e.*, element-wise operation, scaling,  $1 \times 1$  Conv layer and BN layer.

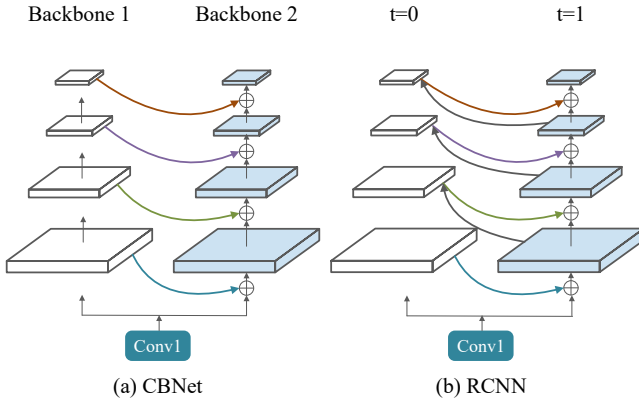


Fig. 3. Comparison between our proposed CBNet architecture ( $K = 2$ ) and the unrolled architecture of RCNN [19] ( $T = 2$ ).

In addition to the above Convolutional Neural Network (CNN)-based detectors, Transformer [15] has been utilized for detection. DETR [34] proposes a fully end-to-end detector by combining CNN and Transformer encoder-decoders. Swin Transformer [17] proposes a general-purpose Transformer backbone to reduce computational complexity and achieves tremendous success in object detection.

**Backbone for Object detection.** Starting from AlexNet [2], deeper and wider backbones have been exploited by mainstream detectors, such as VGG [10], ResNet [11], DenseNet [12], ResNeXt [13], Res2Net [14]. Since the backbone network is usually designed for classification, whether it is pre-trained on ImageNet and fine-tuned on a given detection dataset, or trained from scratch on the detection dataset, it requires many computational resources and can be difficult to optimize. More recently, two non-trivially designed backbones, *i.e.*, DetNet [35] and FishNet [36], are proposed for object detection. These two backbones are specifically designed for the detection task, and they still need to be pre-trained for classification tasks before training (fine-tuning) the detector based on them. Res2Net [14] achieves impressive results in object detection by representing multi-scale features at a granular level and increases the range of receptive fields for each network layer. In addition to manually designing the backbone architecture, DetNAS [16] uses Neural Architecture Search (NAS) for the design of better backbones for object detection, thereby reducing the cost of manual design. DETR [34] and Swin Transformer [17] utilize Transformer modular to build the backbone and achieve impressive results, though require

expensive pre-training.

It is well known that designing and pre-training a new and powerful backbone requires large computation cost. Alternatively, we propose a more economic and efficient solution to build a more powerful backbone for object detection, by assembling multiple identical existing backbones (*e.g.*, ResNet [11], ResNeXt [13], Res2Net [14], DetNAS [16], and Swin Transformer [17]).

**Recurrent Convolution Neural Network.** Different from the feed-forward architecture of CNN, a recurrent CNN (RCNN) [19] incorporates recurrent connections into each convolution layer. This property enhances the ability of the model to integrate the context information, which is important for object recognition. As shown in Fig. 3, our proposed Composite Backbone Network shares some similarities with an unfolded RCNN [19] in terms of architecture, but the two are very different. First, as illustrated in Fig. 3, the connections between the parallel stages are one-way in CBNet, but two-way in RCNN. Second, in RCNN, the parallel stages of different time steps share the parameter weights, while in the proposed CBNet, the parallel stages of backbones are independent of each other. Moreover, if we use RCNN as the backbone for a detector, we need to pre-train it on ImageNet. By contrast, no extra pre-training for CBNetV2 is needed, since it instead uses existing pre-trained weights directly.

### 3 PROPOSED METHOD

This section elaborates the proposed CBNetV2 in detail. We first describe its architecture and variants in Sec. 3.1 and Sec. 3.2 respectively. And then, we describe the structure of detection network with CBNetV2 in Sec. 3.4.

#### 3.1 Architecture of CBNetV2

The architecture of the proposed CBNetV2 is composed of  $K$  identical backbones ( $K \geq 2$ ). In particular, we call the case of  $K = 2$  (shown in Fig. 3.a) as **Dual-Backbone (DB)**, and the case of  $K=3$  as **Triple-Backbone (TB)**.

As illustrated in Fig. 1, the CBNetV2 architecture includes two types of backbones: lead backbone  $B_K$  and assisting backbones  $B_1, B_2, \dots, B_{K-1}$ . Each backbone comprises  $L$  stages (usually  $L = 5$ ), and each stage consists of several convolutional layers with feature maps of the same size. The  $l$ -th stage of the backbone realizes the non-linear transformation  $F^l(\cdot)$  ( $l = 1, 2, \dots, L$ ).

Most traditional convolutional networks follow the design that encodes input images into intermediate features with monotonically decreased resolutions. In particular, the  $l$ -th stage takes the

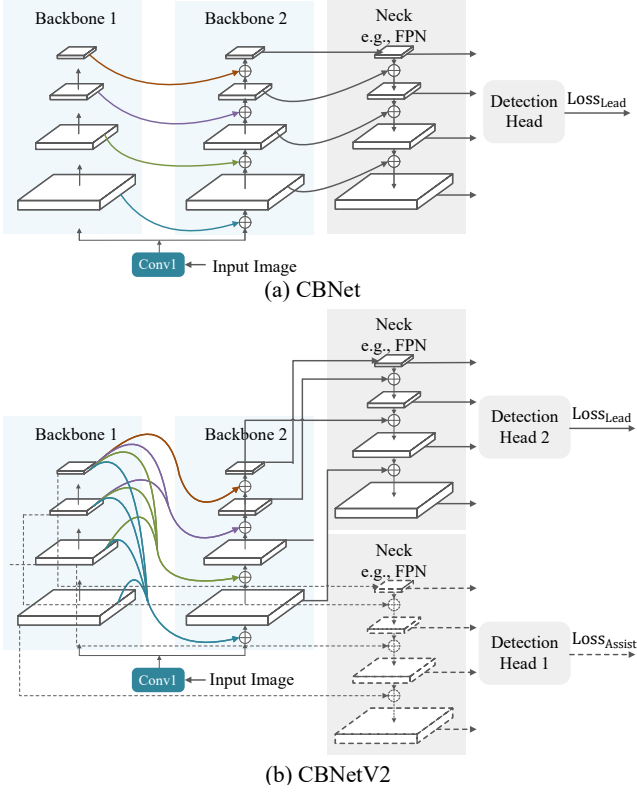


Fig. 4. (a) CBNNet [1] ( $K=2$ ). (b) CBNNetV2 ( $K=2$ ) with the Assistant Supervision. The two FPNs and detection heads share the same weights.

output (denoted as  $x^{l-1}$ ) of the previous  $(l-1)$ -th stage as input, which can be expressed as:

$$x^l = F^l(x^{l-1}), l \geq 2. \quad (1)$$

Differently, we adopt assisting backbones  $B_1, B_2, \dots, B_{K-1}$  to enhance representative ability of lead backbone  $B_K$ . We feed the features of a backbone iteratively to its succeeding backbone in a stage-by-stage fashion. Thus, Equation (1) can be rewritten as:

$$x_k^l = F_k^l(x_k^{l-1} + g^{l-1}(x_{k-1})), l \geq 2, k = 2, 3, \dots, K, \quad (2)$$

where  $g^{l-1}(\cdot)$  represents the composite connection, which takes features (denoted as  $\mathbf{x}_{k-1} = \{x_{k-1}^i | i = 1, 2, \dots, L\}$ ) from assisting backbone  $B_{k-1}$  as input, and a feature of the same size as  $x_k^{l-1}$  as output. Therefore, the output features of  $B_{k-1}$  are transformed and contribute to the input of each stage in  $B_k$ .

For object detection task, only the output features of Lead Backbone  $\{x_K^i, i = 2, 3, \dots, L\}$  are fed into the Neck and then RPN/detection head, while the outputs of assisting backbone are forwarded to its succeeding backbone. It is worth noting that, the  $B_1, B_2, \dots, B_{K-1}$  in CBNNetV2 can adopt various backbone architectures (e.g., ResNet [11], ResNeXt [13], Res2Net [14], DetNAS [16] and Swin Transformer [17]), and is initialized directly from the pre-trained weights of the single backbone.

### 3.2 Possible Composite Styles

For composite connection  $g^l(x)$  that takes  $x = \{x^i | i = 1, 2, \dots, L\}$  from an assisting backbone as input, and outputs a feature of the same size of  $x^l$  ( $k$  is omitted for simplicity), we propose the following five different composite styles.

#### 3.2.1 Same Level Composition (SLC)

An intuitive and simple composite style is to fuse the output features from the same stage of backbones. As shown in Fig. 2.a, the operation of Same Level Composite (SLC) can be formulated as:

$$g^l(x) = \mathbf{w}(x^l), l \geq 2, \quad (3)$$

where  $\mathbf{w}$  represents a  $1 \times 1$  convolution layer and a batch normalization layer.

#### 3.2.2 Adjacent Higher-Level Composition (AHLC)

Motivated by Feature Pyramid Networks [20], the top-down pathway introduces the spatially coarser, but semantically stronger, higher-level features to enhance the lower-level features from the bottom-up pathway. In the previous CBNNet [1], we conduct the Adjacent Higher-Level Composition (AHLC) to feed the output of the adjacent higher-level stage of the previous backbone to the succeeding backbone:

$$g^l(x) = \mathbf{U}(\mathbf{w}(x^{l+1})), l \geq 1, \quad (4)$$

where  $\mathbf{U}(\cdot)$  denotes the up-sample operation. Fig. 2.b illustrates the structure of AHLC.

#### 3.2.3 Adjacent Lower-Level Composition (ALLC)

Contrary to AHLC, we introduce a bottom-up pathway to feed the output of the adjacent lower-level stage of the previous backbone to the succeeding backbone. This operation of Adjacent Lower-Level Composition (ALLC) is shown in Fig. 2.c, which can be formulated as:

$$g^l(x) = \mathbf{D}(\mathbf{w}(x^{l-1})), l \geq 2, \quad (5)$$

where  $\mathbf{D}(\cdot)$  denotes the down-sample operation.

#### 3.2.4 Dense Higher-Level Composition (DHLC)

In DenseNet [12], each layer is connected to all subsequent layers to build comprehensive features. Inspired by it, we utilize dense composite connection in our CBNNet architecture. The operation of DHLC is expressed as following:

$$g^l(x) = \sum_{i=l+1}^L \mathbf{U}(\mathbf{w}_i(x^i)), l \geq 1. \quad (6)$$

As shown in Fig. 2.d, when  $K = 2$ , we compose the features from all the higher-level stages in assisting backbone and add them to the lower-level stage in lead backbone.

#### 3.2.5 Full-connected Composition (FCC)

Different from DHLC, we compose features from all the stages in assisting backbones and feed them to each stage in lead backbone. As shown in Fig. 2.e, we add connections in low-high-level case comparing th DHLC. The operation of DHLC can be expressed as:

$$g^l(x) = \sum_{i=2}^L \mathbf{I}(\mathbf{w}_i(x^i)), l \geq 1, \quad (7)$$

where  $\mathbf{I}(\cdot)$  denotes scale-resizing,  $\mathbf{I}(\cdot) = \mathbf{D}(\cdot)$  when  $i > l$ , and  $\mathbf{I}(\cdot) = \mathbf{U}(\cdot)$  when  $i < l$ .

TABLE 1

Comparison with results using different backbones on the COCO  $\text{test-dev}$  set. \* indicates method with multi-scale testing. "(x+12)" denotes the detectors are trained for an extra 12 epochs using SWA [37].

|                   | Method                                     | AP <sup>box</sup> | AP <sup>box</sup> <sub>50</sub> | AP <sup>box</sup> <sub>75</sub> | AP <sup>box</sup> <sub>S</sub> | AP <sup>box</sup> <sub>M</sub> | AP <sup>box</sup> <sub>L</sub> | Params      | Epochs            |
|-------------------|--|-------------------|---------------------------------|---------------------------------|--------------------------------|--------------------------------|--------------------------------|-------------|-------------------|
| anchor-free-based | FSAF* [25]                                 | 44.6              | 65.2                            | 48.6                            | 29.7                           | 47.1                           | 54.6                           | 94 M        | 24                |
|                   | FCOS [26]                                  | 44.7              | 64.1                            | 48.4                            | 27.6                           | 47.5                           | 55.6                           | 90 M        | 24                |
|                   | DETR-DC5 [34]                              | 44.9              | 64.7                            | 47.7                            | 23.7                           | 49.5                           | 62.3                           | <b>60 M</b> | 500               |
|                   | NAS-FCOS [30]                              | 46.1              | -                               | -                               | -                              | -                              | -                              | 89 M        | 24                |
|                   | GFL [27]                                   | 48.2              | 67.4                            | 52.6                            | 29.2                           | 51.7                           | 60.2                           | 53 M        | 24                |
|                   | ATSS* [6]                                  | 50.7              | 68.9                            | 56.3                            | 33.2                           | 52.9                           | 62.4                           | 95 M        | 24                |
|                   | Deformable DETR* [38]                      | 52.3              | 71.9                            | 58.1                            | 34.4                           | 54.4                           | 65.6                           | -           | 50                |
|                   | <b>Dual-Res2Net101-DCN (ATSS)</b>          | <b>52.8</b>       | <b>71.1</b>                     | <b>57.8</b>                     | <b>35.7</b>                    | <b>56.6</b>                    | <b>63.2</b>                    | 107 M       | <b>32 (20+12)</b> |
| anchor-based      | Auto-FPN [33]                              | 44.3              | -                               | -                               | -                              | -                              | -                              | 90 M        | 24                |
|                   | SM-NAS:E5 [32]                             | 45.9              | 64.6                            | 49.6                            | 27.1                           | 49.0                           | 58.0                           | -           | 24                |
|                   | NAS-FPN [22]                               | 48.3              | -                               | -                               | -                              | -                              | -                              | -           | 150               |
|                   | SP-NAS [39]                                | 49.1              | 67.1                            | 53.5                            | 31                             | 52.6                           | 63.7                           | -           | 50                |
|                   | SpineNet-190 [31]                          | 52.1              | 71.8                            | 56.5                            | 35.4                           | 55                             | 63.6                           | 164 M       | 250               |
|                   | DyHead [40]                                | 54.0              | 72.1                            | 59.3                            | 37.1                           | 57.2                           | 66.3                           | -           | 24                |
|                   | EfficientDet-D7x [23]                      | 55.1              | 74.3                            | 59.9                            | -                              | -                              | -                              | <b>77 M</b> | 600               |
|                   | YOLOv4-P7 [41]                             | 55.5              | 73.4                            | 60.8                            | 38.4                           | 59.4                           | 67.7                           | 288 M       | 450               |
|                   | <b>Dual-Res2Net101-DCN (Cascade R-CNN)</b> | <b>55.3</b>       | <b>73.7</b>                     | <b>60.9</b>                     | <b>37.6</b>                    | <b>58.4</b>                    | <b>67.0</b>                    | 147 M       | <b>32 (20+12)</b> |

### 3.3 The Assistant Supervision

Deep networks lead to good performance [11]. However, increasing the depth of the network may introduce additional optimization difficulty as shown in [42] for image classification. [43], [44] introduce the auxiliary classifiers of intermediate layers to improve the convergence of very deep networks. In original CBNet, although the composite backbones are in parallel, the latter backbones (*e.g.*, lead backbone in Fig. 4.a) deepen the network through adjacent connections between the previous backbone (*e.g.*, assisting backbone in Fig. 4.a). For the better training of CBNet-based detectors, We propose to generate initial results of assisting backbones by supervision with an auxiliary detection head to provide additional regularization.

An example of our supervised CBNetV2 is illustrated in Fig. 4.b. Apart from the original loss using lead backbone feature to train the detection head 1, another detection head 2 takes assisting backbone features as input to produce the Assistant Supervision. Note that detection head 1 and detection head 2 are weight sharing. The assistant supervision helps optimize the learning process, while the original loss for lead backbone takes the most responsibility. We add weight to balance the Assistant Supervision, where the total loss is represented as:

$$\mathcal{L} = \mathcal{L}_{\text{Lead}} + \sum_{i=1}^{K-1} (\lambda_i * \mathcal{L}_{\text{Assist}}^i). \quad (8)$$

where  $\mathcal{L}_{\text{Lead}}$  is the loss of lead backbone,  $\mathcal{L}_{\text{Assist}}$  is the loss of assisting backbones, and  $\lambda_i$  is the loss weight for each assisting backbone.

In particular, during the inference stage, we abandon the assistant supervision branch and only utilize the output feature of lead backbone in CBNetV2 (Fig. 4.b). The Assistant Supervision does not affect the speed of the inference stage.

### 3.4 Architecture of Detection Network with CBNetV2

The CBNetV2 architecture applies to various off-the-shelf object detectors without additional modifications to the network architectures. In practice, we attach layers of lead backbone with functional networks, FPN [20], RPN [4], detection head [4],

[7], [8], [21], [28]. The inference stage of CBNetV2 for object detection is shown in Fig. 1.

## 4 EXPERIMENTS

### 4.1 Implementation details

#### 4.1.1 Datasets and Evaluation Criteria

We conduct experiments on the COCO [18] benchmark. The training is conducted on the 118k training images, and ablation studies are evaluated on the 5k minimal images. We also report the results on the 20k images in  $\text{test-dev}$  for comparison with state-of-the-art (SOTA). For evaluation, we adopt the metrics from the COCO detection evaluation criteria, including the mean Average Precisions (AP) across IoU thresholds ranging from 0.5 to 0.95 at different scales.

#### 4.1.2 Training and Inference Details

Our experiments are based on open source detection toolbox MMDetection [49]. For ablation studies and simple comparisons, we resize input size to  $800 \times 500$  during training and inference if not specified. We choose Faster R-CNN (ResNet50 [11]) with FPN [20] as the baseline. We use SGD optimizer with initial learning rate 0.02 (0.01 for Res2Net), momentum 0.9, and  $10^{-4}$  as weight decay. We train detectors for 12 epochs with a batch size of 16, we only use random flip for data augmentation. Note that some of the conclusions are slightly different from CBNet [1] since we use MMDetection instead of Caffe2 [50] in this paper. Different development environments may cause different experimental results. In particular, if not specifically highlighted, the experiments related to Swin Transformer follow the hyperparameters of the original paper [17].

For comparison with state-of-the-art detectors (Table 1 and 2), we utilize multi-scale training [51] (short side resized to  $400 \sim 1400$  and long side is at most 1600) for 20 epochs with learning rate decayed by  $10 \times$  at epoch 16 and 19. Notably, following [17],  $3 \times$  schedule (36 epochs with the learning rate decayed by  $10 \times$  at epochs 27 and 33) is used for Dual-Swin-S. Some detectors are trained for an extra 12 epochs using Stochastic Weights Averaging (SWA) [37]. During inference, we use Soft-NMS [52] with a threshold of 0.001, and the input size is set to  $1600 \times 1400$ . All

TABLE 2

Comparison between our methods and state-of-the-art detectors on COCO object detection and instance segmentation. \* indicates multi-scale testing. "(x+12)" denotes the detectors are trained for an extra 12 epochs using SWA [37].

| Pre-trained on       | Method                                  | mini-val          |                    | test-dev          |                    | Params       | Epochs            |
|----------------------|---|-------------------|--------------------|-------------------|--------------------|--------------|-------------------|
|                      |   | AP <sup>box</sup> | AP <sup>mask</sup> | AP <sup>box</sup> | AP <sup>mask</sup> |              |                   |
| ImageNet-1K          | GCNet* [45]                             | 51.8              | 44.7               | 52.3              | 45.4               | -            | 36                |
|                      | Swin-B [17]                             | 51.9              | 45.0               | -                 | -                  | 145 M        | 36                |
|                      | ResNeSt-200* [46]                       | 52.5              | -                  | 53.3              | 47.1               | -            | 36                |
|                      | <b>Dual-Swin-S (Cascade Mask R-CNN)</b> | <b>56.3</b>       | <b>48.6</b>        | <b>56.9</b>       | <b>49.1</b>        | <b>156 M</b> | <b>36</b>         |
| ImageNet-1K&JFT [47] | CopyPaste [48]                          | 55.9              | 47.2               | 56.0              | 47.4               | 185 M        | 96                |
| ImageNet-22K         | Swin-L (HTC++) [17]                     | 57.1              | 49.5               | 57.7              | 50.2               | 284 M        | 72                |
|                      | <b>Dual-Swin-B (HTC)</b>                | <b>57.9</b>       | <b>50.2</b>        | -                 | -                  | <b>231 M</b> | <b>20</b>         |
|                      | <b>Dual-Swin-B (HTC)</b>                | <b>58.2</b>       | <b>50.4</b>        | <b>58.6</b>       | <b>51.1</b>        | <b>231 M</b> | <b>32 (20+12)</b> |
|                      | Swin-L (HTC++) [17]*                    | 58.0              | 50.4               | 58.7              | 51.1               | 284 M        | 72                |
|                      | <b>Dual-Swin-B (HTC)*</b>               | <b>58.9</b>       | <b>51.2</b>        | <b>59.3</b>       | <b>51.8</b>        | <b>231 M</b> | <b>32 (20+12)</b> |

TABLE 3

Comparison of Dual-Backbone with a single backbone in terms of different architectures. Input size is  $800 \times 500$  for training, inference and GFLOPs computation.

| Backbone                    | AP <sup>box</sup> | Params | FLOPs |
|-----------------------------|-------------------|--------|-------|
| ResNet50                    | 34.6              | 41.5 M | 90 G  |
| <b>Dual-ResNet50</b>        | <b>38.1</b>       | 69.7 M | 127 G |
| ResNeXt50-32x4d             | 36.3              | 41.0 M | 91 G  |
| <b>Dual-ResNeXt50-32x4d</b> | <b>39.4</b>       | 68.6 M | 129 G |
| Res2Net50                   | 37.7              | 41.7 M | 94 G  |
| <b>Dual-Res2Net50</b>       | <b>41.3</b>       | 70.0 M | 132 G |
| DetNAS-1.3G                 | 36.1              | 26.1 M | 66 G  |
| <b>Dual-DetNAS-1.3G</b>     | <b>37.8</b>       | 35.6 M | 77 G  |

other hyper-parameters in this paper follow MMDetection if not specified.

## 4.2 Main Results

### 4.2.1 Comparison with State-of-the-Art

**Object Detection.** We compare our methods with cutting edge detectors. As shown in Table 1, we summarize them into two categories: anchor-based, and anchor-free-based. We select ATSS [6] as our anchor-free representative, and Cascade R-CNN and as our anchor-based representative. Compared with methods with only bounding box annotations training, our ATSS Dual-Res2Net101-DCN achieves 52.8% AP, outperforming previous anchor-free methods [6], [25], [26], [27], [30], [34], [38], including their multi-scale testing results; for anchor-based detectors [22], [23], [31], [32], [33], [39], [40], [41], our Cascade R-CNN Dual-Res2Net101-DCN achieves a comparable result of 55.3% AP. It is worth noting that some detectors (*i.e.*, EfficientDet) require extremely expensive training costs, *i.e.*, large batch-size (128) with a long training schedule (600 epochs), while our CBNetV2 trains only for 32 epochs with batch-size of 8.

**Instance Segmentation.** We further compare our method with state-of-the-art results [17], [45], [46], [48] with using both bounding box and instance segmentation annotations in Table 2. Using Cascade Mask R-CNN, our Dual-Swin-S achieves 56.3% box AP and 48.6% mask AP on COCO *minival* in terms of the bounding box and instance segmentation, which are significant gains of +4.4% box AP and +3.6% mask AP over Swin-B with similar model size, surpassing other ImageNet-1K pre-trained backbone-based detectors. Without whistles and bells, our

HTC Dual-Swin-B (Swin-B [17] is pre-trained on ImageNet22K) achieves single-model single-scale result of 57.9% box AP and 50.2% mask AP on COCO *minival*, which are 0.8% box AP and 0.9% mask AP higher than that of Swin-L (HTC++) with 19% less parameter amount and much shorter training schedules (*e.g.*, 20 vs. 72 epochs). Particularly, with 12 more epochs training using SWA, we achieve 58.6% box AP and 51.1% mask AP on COCO *test-dev*, outperforming prior art. We can push the current best single model result to a new record of 59.3% box AP and 51.8% mask AP without extra training data through multi-scale testing. These results demonstrate the effectiveness of our carefully designed composite backbone.

### 4.2.2 Generality for Main-stream Backbone Architectures

CBNetV2 expands the receptive field by combining backbones in parallel, rather than simply increasing the depth of backbones. To demonstrate the effectiveness of our design strategy, we conduct experiments on Faster R-CNN, with different backbone architectures. As shown in Table 3, Dual-Res2Net50 increases Res2Net50 by 3.6% AP to 41.3% AP. As for other backbones (*e.g.*, ResNet, ResNeXt-32x4d), our method can boost baseline by over 3% AP. Even for the searched backbone DetNAS, our CBNetV2 can still improve baseline by 1.7% AP.

Note that compared with the baseline, the number of parameters of CBNetV2 has increased. To better demonstrate the effectiveness of composite architecture, we compare CBNetV2 with deeper and wider backbone networks. As shown in Table 4, with fewer FLOPs/Params (*e.g.*, FLOPs 127G vs. 151 G, Params 69.7 M vs. 76.2 M), Dual-ResNet50 is 0.3% AP higher than that of the deeper ResNet152. Furthermore, Dual-ResNeXt50-32x4d is 0.7% AP higher than that of ResNeXt101-64x4d with only 70% parameter amount. Dual-DetNAS-1.3G is 0.4% AP higher than that of DetNAS-3.8G with 9.2 M less number of parameters. Results demonstrate that our composite backbone architecture is more efficient and effective than simply increasing the depth of the network.

### 4.2.3 Model Compatibility with Deformable Convolution

Deformable convolution [53] enhances the transformation modeling capability of CNNs and is widely used for accurate object detectors (*e.g.*, simply adding DCN improves Faster R-CNN ResNet50 from 34.6% to 37.4% AP). To show the compatibility of our CBNetV2 architecture with deformable convolution, we conduct experiments on Faster R-CNN ResNet50-DCN. As shown in

TABLE 4

Comparison of Dual-Backbone with a deeper single backbone in terms of different architectures.

| Backbone                    | AP <sup>box</sup> | Params        | FLOPs        |
|-----------------------------|-------------------|---------------|--------------|
| ResNet101                   | 36.3              | 60.5 M        | 121 G        |
| ResNet152                   | 37.8              | 76.2 M        | 151 G        |
| <b>Dual-ResNet50</b>        | <b>38.1</b>       | <b>69.7 M</b> | <b>127 G</b> |
| ResNeXt101-32x4d            | 37.7              | 60.2 M        | 122 G        |
| ResNeXt101-64x4d            | 38.7              | 99.3 M        | 183 G        |
| <b>Dual-ResNeXt50-32x4d</b> | <b>39.4</b>       | <b>68.6 M</b> | <b>129 G</b> |
| Res2Net101                  | 40.1              | 61.2 M        | 125 G        |
| Res2Net200                  | 41.7              | 92.2 M        | 185 G        |
| <b>Dual-Res2Net50</b>       | <b>41.3</b>       | <b>70.0 M</b> | <b>132 G</b> |
| DetNAS-3.8G                 | 37.4              | 44.8 M        | 89 G         |
| <b>Dual-DetNAS-1.3G</b>     | <b>37.8</b>       | <b>35.6 M</b> | <b>77 G</b>  |

TABLE 5

The compatibility of CBNetV2 and deformable convolution.

| Backbone                   | AP <sup>box</sup> |             | $\Delta$ AP <sup>box</sup> |
|----------------------------|-------------------|-------------|----------------------------|
|                            | w/o DCN           | w/ DCN      |                            |
| ResNet50                   | 34.6              | 37.4        | +2.8                       |
| ResNet152                  | 37.8              | 39.8        | +2.0                       |
| <b>Dual-ResNet50</b>       | <b>38.1</b>       | <b>40.4</b> | <b>+2.3</b>                |
| ResNeXt50-32x4d            | 36.3              | 38.6        | +2.3                       |
| ResNeXt101-64x4            | 38.7              | 41.0        | +2.3                       |
| <b>Dual-ResNeXt50-32x4</b> | <b>39.4</b>       | <b>42.3</b> | <b>+2.9</b>                |

Table 5, DCN is still effective on Dual-ResNet50 Dual-ResNeXt50-32x4d with 2.3% AP and 2.9% AP improvement, respectively. The improvement is larger than the 2.0% AP and 1.3% AP increments on ResNet152 and ResNeXt101-64x4d. Dual-ResNet50-DCN increases ResNet50-DCN by 3.0% AP and is 0.6% higher than that of the deeper ResNet152-DCN. Also, Dual-ResNet50-32x4d-DCN increases ResNet50-32x4d-DCN by 3.7% AP, which is 1.3% higher than that of the deeper and wider ResNeXt101-64x4d-DCN. The results show that the effects of CBNetV2 and deformable convolution can be superimposed without conflicting with each other.

#### 4.2.4 Model Adaptability for Mainstream Detectors

To further verify the performance of CBNetV2 on main-stream detectors, we apply it to a one-stage detector (RetinaNet), anchor-free detector (ATSS), two-stage detectors (Faster R-CNN, Mask R-CNN, and Cascade R-CNN) in Table 6. Under the same strategy with baseline, we obtain a much better performance on each detector: CBNetV2 improves RetinaNet and ATSS by 3% AP, Faster R-CNN by 3.3% AP, and improves Cascade R-CNN by 3% AP. The instance segmentation is also improved by 2.9% AP for Mask R-CNN. The results demonstrate the model adaptability of CBNetV2. Our CBNetV2 can be flexibly plugged into mainstream detectors and improve the performance by a large margin. The results convey that our CBNetV2 is suitably designed for object detection.

#### 4.2.5 Model Adaptability for Swin Transformer

Transformer is notable for its use of attention to model long-range dependencies in the data; Swin Transformer [17] is one of the most representative recent arts. It proposes a general-purpose Transformer backbone, which constructs hierarchical feature APs and has linear computational complexity in image size. We conduct

TABLE 6

Comparison of Dual-Backbone with a single backbone in terms of different detectors.

| Detector      | Backbone             | AP <sup>box</sup> | AP <sup>mask</sup> | Params | FLOPs |
|---------------|----------------------|-------------------|--------------------|--------|-------|
| RetinaNet     | ResNet50             | 33.2              | -                  | 37.7 M | 95 G  |
|               | <b>Dual-ResNet50</b> | <b>36.2</b>       | -                  | 65.9 M | 131 G |
| ATSS          | ResNet50             | 36.9              | -                  | 32.1 M | 81 G  |
|               | <b>Dual-ResNet50</b> | <b>39.9</b>       | -                  | 64.3 M | 118 G |
| Faster R-CNN  | ResNet50             | 34.6              | -                  | 41.5 M | 90 G  |
|               | <b>Dual-ResNet50</b> | <b>38.1</b>       | -                  | 69.7 M | 127 G |
| Mask R-CNN    | ResNet50             | 35.2              | 31.8               | 44.2 M | 159 G |
|               | <b>Dual-ResNet50</b> | <b>39.0</b>       | <b>34.7</b>        | 72.3 M | 195 G |
| Cascade R-CNN | ResNet50             | 38.2              | -                  | 69.2 M | 118 G |
|               | <b>Dual-ResNet50</b> | <b>41.2</b>       | -                  | 97.3 M | 155 G |

TABLE 7

Results on COCO minival object detection and instance segmentation.

| Detector   | Backbone           | AP <sup>box</sup> | AP <sup>mask</sup> | Params  | FLOPs |
|------------|--------------------|-------------------|--------------------|---------|-------|
| Cascade    | Swin-T             | 50.5              | 43.7               | 85.6 M  | 742 G |
|            | Swin-S             | 51.8              | 44.7               | 107.0 M | 832 G |
| Mask R-CNN | Swin-B             | 51.9              | 45.0               | 145.0 M | 975 G |
|            | <b>Dual-Swin-T</b> | <b>53.6</b>       | <b>46.2</b>        | 113.8 M | 836 G |

experiments on Swin Transformer to convey the model adaptability of CBNetV2. For fair comparisons, we follow the same training strategy as [17] with multi-scale training (the short side resized to 480 ~ 800 and the long side is at most 1333), AdamW optimizer (initial learning rate of 0.0001, weight decay of 0.05, and batch size of 16), and 3x schedule (36 epochs with the learning rate decayed by 10x at epochs 27 and 33). As shown in Table 7, as the Swin Transformer continues to deepen, the accuracy of the model slowly improves and reaches saturation at Swin-S. Swin-B is only 0.1% AP higher than that of Swin-S, but the parameter amount increases by 38 M. While performing Dual-Swin-T, we achieve 53.6% box AP and 46.2% mask AP by improving Swin-T 3.1% box AP and 2.5% mask AP. Surprisingly, our Dual-Swin-T is 1.7% box AP and 1.2% mask AP higher than that of the deeper and wider Swin-B with fewer FLOPs/Params (e.g., FLOPs 836 G vs. 975 G, Params 113.8 M vs. 145.0 M). These results prove that CBNetV2 also has a strong improvement effect on non-pure convolutional architectures. The experiment also gives strong evidence that even on large high-precision detectors, CBNetV2 is more effective than simply increasing the network depth and width.

### 4.3 Ablation studies

We ablate various design choices for our proposed CBNetV2. For simplicity, all accuracy results here are for the COCO validation set with 800 × 500 input size if not specified.

#### 4.3.1 Ablation studies on different composite styles

We conduct experiments to compare the suggested composite styles illustrated in Fig. 2, including SLC, AHLC, ALLC, DHL C and FCC. All of these experiments are conducted based on the Faster R-CNN Dual-ResNet50 architecture; we use Faster R-CNN ResNet50 as the baseline.

SLC As presented in Table 8, SLC gets an even worse result than that of the single-backbone baseline. We speculate that this is because the SLC architecture brings serious parameter

TABLE 8  
Comparison between different composite styles.

| Composite style | AP <sup>box</sup> | Params  | FLOPs |
|-----------------|-------------------|---------|-------|
| -               | 34.6              | 41.5 M  | 90 G  |
| SLC             | 35.0              | 64.81 M | 123 G |
| AHLC            | 36.0              | 67.6 M  | 148 G |
| ALLC            | 32.4              | 67.6 M  | 156 G |
| <b>DHLC</b>     | <b>37.3</b>       | 69.7 M  | 150 G |
| <b>FCC</b>      | <b>37.4</b>       | 72.0 M  | 168 G |

TABLE 9  
Different loss weights for supervision of assisting backbone.

| # Backbones | $\lambda_1$ | $\lambda_2$ | AP <sup>bbox</sup> |
|-------------|-------------|-------------|--------------------|
| Dual        | 0           | -           | 37.3               |
|             | 0.125       | -           | 37.6               |
|             | 0.25        | -           | 37.9               |
|             | <b>0.5</b>  | -           | <b>38.1</b>        |
|             | 1.0         | -           | 38.0               |
| Triple      | 0           | 0           | 37.4               |
|             | 0.25        | 0.25        | 37.9               |
|             | 0.25        | 0.5         | 38.9               |
|             | 0.5         | 0.5         | 38.6               |
|             | <b>0.5</b>  | <b>1.0</b>  | <b>39.1</b>        |

redundancy. More specifically, the features extracted by the same stage of the two backbones are similar, hence SLC cannot learn more semantic information than a single backbone do.

**AHLC** As presented in Table 8, the simple top-down pathway introduced by AHLC improves baseline by 1.4% AP, which verifies our motivation in Sec. 3.2.2.

**ALLC** As shown in Table 8, ALLC drops the performance of baseline by 1.4% AP. We infer that if we directly add the lower-level (i.e., shallower) features of assisting backbone to the higher-level (i.e., deeper) ones of lead backbone, the semantic information of the later ones will be largely harmed. On the contrary, if the higher-level features of assisting backbone are fed to the lower-level stages of lead backbone, the semantic information of the latter ones can be enhanced.

**DHLC** The results in Table 8 show that DHLC improves the performance of baseline by a large margin (from 34.6% AP to 37.3% AP by 2.7% AP). More composite connections of the high-low cases enrich the representation ability of features to some extent.

**FCC** According to Table 8, FCC achieves the best performance of 37.4% AP thanks to the fully connected architecture.

From the observed experiments, FCC and DHLC achieved the top two results. Considering the simplicity of calculation, we use DHLC as the default composite style of CBNetV2. All above composite styles share a similar amount of parameters, but the accuracy varies greatly. These results prove that only increasing the number of parameters or adding additional backbones do not guarantee better results. Also, composite connections are key to compose backbones. These results demonstrate that the suggested DHLC composite style is effective and nontrivial.

#### 4.3.2 Ablation studies on the Assistant Supervision

Experimental results related to weighting the Assistant Supervision are presented in Table 9. For simplicity, we conduct experiments on CBNetV2 with DHLC composite style. The first setting is the Faster R-CNN Dual-ResNet50 baseline and the second is

TABLE 10  
Comparing the Composite Backbone, the DHLC composite style and the Assistant Supervision

| # Backbones   | DHLC | Supervision | AP <sup>bbox</sup> |
|---------------|------|-------------|--------------------|
| <b>Single</b> |      |             | 34.6               |
|               |      |             | 36.0               |
| Dual          | ✓    |             | 37.3               |
|               |      | ✓           | 36.9               |
|               | ✓    | ✓           | <b>38.1</b>        |
|               |      |             | 36.4               |
| Triple        | ✓    |             | 37.4               |
|               |      | ✓           | 37.5               |
|               | ✓    | ✓           | <b>39.1</b>        |

the Triple-ResNet50 baseline, where  $\lambda$  for assisting backbone in Equation (8) is set as zero. For the Dual-Backbone (DB) structure, the baseline can be improved by 0.9% AP by setting  $\lambda_1$  as 0.5. For the Triple-Backbone (TB) structure, the baseline can be improved by 1.5% AP by setting  $\{\lambda_1, \lambda_2\}$  as  $\{0.25, 0.5\}$ . The experimental results verify that the Assistant Supervision forms an effective training strategy and improves the performance of CBNetV2.

#### 4.3.3 Ablation studies on the importance of each component

To further analyze the importance of each component in CBNetV2, the Composite Backbone, the DHLC composite style, and the Assistant Supervision are gradually applied to the model to validate the effectiveness. Meanwhile, the improvements brought by the combination of different components are also presented to demonstrate that these components are complementary to each other. The baseline is Faster R-CNN with ResNet50 as a single backbone. All the results are shown in Table 10.

As shown in Table 10, the Dual-Backbone (DB) and Triple-Backbone (TB) with AHLC default composite style improve the baseline by 1.4% and 1.8% AP, respectively. It verifies the effectiveness of our composite backbone structure (CBNet [1]). The DHLC composite style further improves the detection performance of DB and TB by over 1.0% AP. The results indicate that DHLC enables larger receptive fields, where each level feature receives rich semantic information from all higher-level features. The Assistant Supervision brings about 1.0% AP increment in DB and TB, which benefits from the supervision for assisting backbones forming a better training strategy and improving the representative ability of lead backbone. It is worth noting that the Assistant Supervision does not introduce extra parameters in the inference stage. When combining three components, there is a large improvement over the baseline method. The DHLC-style DB and TB with the Assistant Supervision achieves 37.9% AP and 38.9% AP, respectively, and improves the baseline by 3.3% AP and 4.3% AP, respectively. Also, CBNetV2 improves CBNet [1] by 1.8% and 1.7% AP in terms of DB and TB respectively.

#### 4.3.4 Number of backbones in CBNet

We conduct experiments to investigate the relationship between the number of backbones in CBNetV2 and the detection performance. We choose Faster R-CNN ResNet50 with  $800 \times 500$  input size as the baseline, and the results are shown in Fig. 6. It can be noted that the detection AP steadily increases with the number of backbones, and tends to converge when the number of backbones reaches three. Hence, considering the speed and memory cost, we suggest using Dual-Backbone and Triple-Backbone architectures.

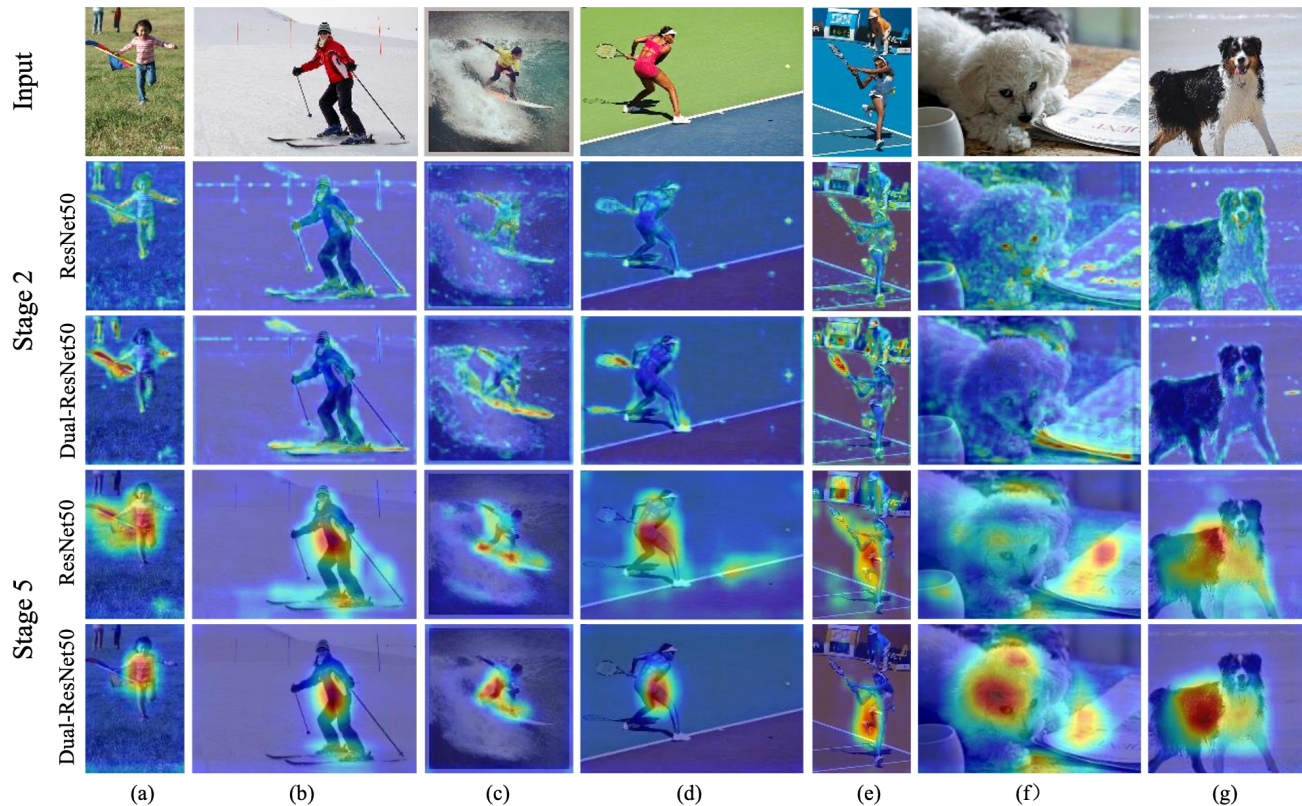


Fig. 5. Visualization of class activation APing, using ResNet50 and Dual-ResNet50 as backbone. The baseline detector is Faster R-CNN ResNet50 with  $800 \times 500$  input size. For each backbone, we visualize the stage 2 and stage 5 features according to the size of the foreground objects. Best viewed in color.

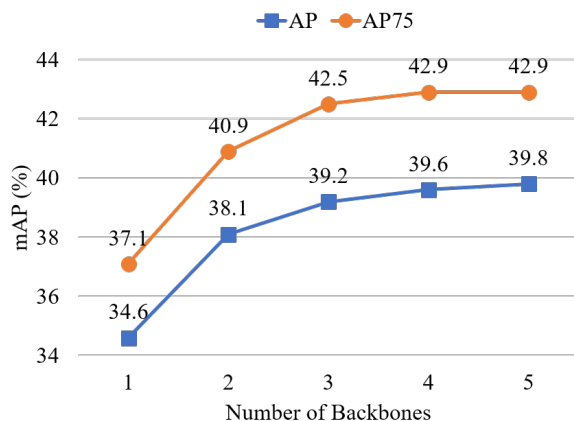


Fig. 6. Comparing the performances of CBNetV2 with different number of composite backbones.

#### 4.4 Class Activation Mapping

To understand the representative ability of CBNetV2, we visualize the class activation mapping (CAM) using Grad-CAM [54], which is commonly used to localize the discriminative regions for image classification and object detection. In the visualization examples shown in Fig. 5, stronger CAM areas are covered with lighter/warmer colors. To better illustrate the multi-scale detection capabilities of CBNetV2, we correspondingly visualize the large-

scale feature APs of stage 2 (for detecting small objects) and the small-scale feature APs of stage 5 (for detecting large objects) extracted by our CBNetV2 and the original single backbone. Compared with the single-backbone of ResNet, the Dual-ResNet based CAM results have more concentrated activation APs on large objects of the stage 5 feature, such as the 'person', 'dog' in Fig. 5, while single backbone only covers parts of objects, or disturbed by the background. On the other hand, CBNetV2 has a stronger ability to distinguish small objects with stage 2 feature, for example, 'kite' in Fig. 5 (a), 'skateboard' in (b), 'surfboard' in (c), and 'tennis racket' in (d,e), while single backbone hardly activates on these parts.

## 5 CONCLUSION

In this paper, we propose a novel network architecture called *Composite Backbone Network V2* (CBNetV2) to boost the performance of cutting edge object detectors. CBNetV2 consists of a series of backbones with the same network architecture in parallel, the DHLC composite strategy, and the assistant supervision. They work together to construct a strong representative backbone network for object detection with existing open-sourced pre-trained weights instead of additional pre-training. Extensive experimental results demonstrate that the proposed CBNetV2 can be flexibly plugged into many mainstream detectors, including one-stage (*e.g.*, RetinaNet) and two-stage (Faster R-CNN, Mask R-CNN, Cascade R-CNN, and Cascade Mask R-CNN) detectors, as well as anchor-based (*e.g.*, Faster R-CNN) and anchor-free-based (*e.g.*, ATSS) ones. Specifically, the performances of the detectors mentioned above are increased by over 3% AP. Furthermore, our

CBNetV2 is more effective and efficient than simply increasing the network depth and width over various backbones, including manual-based (ResNet, ResNeXt, Res2Net) and NAS-based (DetNAS), as well as CNN-based (*e.g.*, ResNet) and Transformer-based (Swin-Transformer) ones. Also, the effects of CBNetV2 and deformable convolution can be superimposed without conflicting with each other. In particular, our Cascade R-CNN Dual-Res2Net101 achieves 55.3% AP, and HTC Dual-Swin-B achieves new records of 58.6% box AP and 51.1% mask AP on COCO *test-dev*, outperforming prior single-model and single-scale results. With multi-scale testing, we achieve a single-model-state-of-the-art result of 59.3% box AP and 51.8% mask AP without extra training data.

## ACKNOWLEDGMENTS

We thank Dr. Han Hu, Prof. Ming-Ming Cheng, and Shang-Hua Gao for the insightful discussions.

## REFERENCES

- [1] Y. Liu, Y. Wang, S. Wang, T. Liang, Q. Zhao, Z. Tang, and H. Ling, "Cbnet: A novel composite backbone network architecture for object detection," in *AAAI*, 2020. **1, 2, 4, 5, 8**
- [2] A. Krizhevsky, I. Sutskever, and G. E. Hinton, "Imagenet classification with deep convolutional neural networks," in *NeurIPS*, 2012. **1, 3**
- [3] W. Liu, D. Anguelov, D. Erhan, C. Szegedy, S. E. Reed, C. Fu, and A. C. Berg, "SSD: single shot multibox detector," in *ECCV*, 2016. **1, 2**
- [4] S. Ren, K. He, R. B. Girshick, and J. Sun, "Faster R-CNN: towards real-time object detection with region proposal networks," *TPAMI*, 2017. **1, 2, 5**
- [5] T. Lin, P. Goyal, R. B. Girshick, K. He, and P. Dollár, "Focal loss for dense object detection," *TPAMI*, 2020. **1, 2**
- [6] S. Zhang, C. Chi, Y. Yao, Z. Lei, and S. Z. Li, "Bridging the gap between anchor-based and anchor-free detection via adaptive training sample selection," in *CVPR*, 2020. **1, 2, 5, 6**
- [7] K. He, G. Gkioxari, P. Dollár, and R. B. Girshick, "Mask R-CNN," in *ICCV*, 2017. **1, 2, 5**
- [8] Z. Cai and N. Vasconcelos, "Cascade R-CNN: delving into high quality object detection," in *CVPR*, 2018. **1, 2, 5**
- [9] J. Deng, W. Dong, R. Socher, L.-J. Li, K. Li, and L. Fei-Fei, "Imagenet: A large-scale hierarchical image database," in *CVPR*, 2009. **1**
- [10] K. Simonyan and A. Zisserman, "Very deep convolutional networks for large-scale image recognition," in *ICLR*, 2015. **1, 3**
- [11] K. He, X. Zhang, S. Ren, and J. Sun, "Deep residual learning for image recognition," in *CVPR*, 2016. **1, 2, 3, 4, 5**
- [12] G. Huang, Z. Liu, L. Van Der Maaten, and K. Q. Weinberger, "Densely connected convolutional networks," in *CVPR*, 2017. **1, 3, 4**
- [13] S. Xie, R. Girshick, P. Dollár, Z. Tu, and K. He, "Aggregated residual transformations for deep neural networks," in *CVPR*, 2017. **1, 2, 3, 4**
- [14] S. Gao, M. Cheng, K. Zhao, X. Zhang, M. Yang, and P. H. S. Torr, "Res2net: A new multi-scale backbone architecture," *TPAMI*, 2021. **1, 2, 3, 4**
- [15] A. Vaswani, N. Shazeer, N. Parmar, J. Uszkoreit, L. Jones, A. N. Gomez, L. Kaiser, and I. Polosukhin, "Attention is all you need," in *NeurIPS*, 2017. **1, 3**
- [16] Y. Chen, T. Yang, X. Zhang, G. Meng, X. Xiao, and J. Sun, "Detnas: Backbone search for object detection," in *NeurIPS*, 2019. **1, 2, 3, 4**
- [17] Z. Liu, Y. Lin, Y. Cao, H. Hu, Y. Wei, Z. Zhang, S. Lin, and B. Guo, "Swin transformer: Hierarchical vision transformer using shifted windows," *arXiv preprint arXiv:2103.14030*, 2021. **2, 3, 4, 5, 6, 7**
- [18] T. Lin, M. Maire, S. J. Belongie, J. Hays, P. Perona, D. Ramanan, P. Dollár, and C. L. Zitnick, "Microsoft COCO: common objects in context," in *ECCV*, 2014. **2, 5**
- [19] M. Liang and X. Hu, "Recurrent convolutional neural network for object recognition," in *CVPR*, 2015. **3**
- [20] T. Lin, P. Dollár, R. B. Girshick, K. He, B. Hariharan, and S. J. Belongie, "Feature pyramid networks for object detection," in *CVPR*, 2017. **2, 4, 5**
- [21] J. Redmon, S. Divvala, R. Girshick, and A. Farhadi, "You only look once: Unified, real-time object detection," in *CVPR*, 2016. **2, 5**
- [22] G. Ghiasi, T. Lin, and Q. V. Le, "NAS-FPN: learning scalable feature pyramid architecture for object detection," in *CVPR*, 2019. **2, 5, 6**
- [23] M. Tan, R. Pang, and Q. V. Le, "Efficientdet: Scalable and efficient object detection," in *CVPR*, 2020. **2, 5, 6**
- [24] J. Pang, K. Chen, J. Shi, H. Feng, W. Ouyang, and D. Lin, "Libra r-cnn: Towards balanced learning for object detection," in *CVPR*, 2019. **2**
- [25] C. Zhu, Y. He, and M. Savvides, "Feature selective anchor-free module for single-shot object detection," in *CVPR*, 2019. **2, 5, 6**
- [26] Z. Tian, C. Shen, H. Chen, and T. He, "FCOS: fully convolutional one-stage object detection," in *ICCV*, 2019. **2, 5, 6**
- [27] X. Li, W. Wang, L. Wu, S. Chen, X. Hu, J. Li, J. Tang, and J. Yang, "Generalized focal loss: Learning qualified and distributed bounding boxes for dense object detection," in *NeurIPS*, 2020. **2, 5, 6**
- [28] S. Zhang, L. Wen, X. Bian, Z. Lei, and S. Z. Li, "Single-shot refinement neural network for object detection," in *CVPR*, 2018. **2, 5**
- [29] K. Duan, S. Bai, L. Xie, H. Qi, Q. Huang, and Q. Tian, "Centernet: Keypoint triplets for object detection," in *ICCV*, 2019. **2**
- [30] N. Wang, Y. Gao, H. Chen, P. Wang, Z. Tian, C. Shen, and Y. Zhang, "NAS-FCOS: fast neural architecture search for object detection," in *CVPR*, 2020. **2, 5, 6**
- [31] X. Du, T. Lin, P. Jin, G. Ghiasi, M. Tan, Y. Cui, Q. V. Le, and X. Song, "Spinenet: Learning scale-permuted backbone for recognition and localization," in *CVPR*, 2020. **2, 5, 6**
- [32] L. Yao, H. Xu, W. Zhang, X. Liang, and Z. Li, "SM-NAS: structural-to-modular neural architecture search for object detection," in *AAAI*, 2020. **2, 5, 6**
- [33] H. Xu, L. Yao, Z. Li, X. Liang, and W. Zhang, "Auto-fpn: Automatic network architecture adaptation for object detection beyond classification," in *ICCV*, 2019. **2, 5, 6**
- [34] N. Carion, F. Massa, G. Synnaeve, N. Usunier, A. Kirillov, and S. Zagoruyko, "End-to-end object detection with transformers," in *ECCV*, 2020. **3, 5, 6**
- [35] Z. Li, C. Peng, G. Yu, X. Zhang, Y. Deng, and J. Sun, "Detnet: Design backbone for object detection," in *ECCV*, 2018. **3**
- [36] S. Sun, J. Pang, J. Shi, S. Yi, and W. Ouyang, "Fishnet: A versatile backbone for image, region, and pixel level prediction," in *NeurIPS*, 2018. **3**
- [37] H. Zhang, Y. Wang, F. Dayoub, and N. Sünderhauf, "Swa object detection," *arXiv preprint arXiv:2012.12645*, 2020. **5, 6**
- [38] X. Zhu, W. Su, L. Lu, B. Li, X. Wang, and J. Dai, "Deformable detr: Deformable transformers for end-to-end object detection," in *ICLR*, 2021. **5, 6**
- [39] C. Jiang, H. Xu, W. Zhang, X. Liang, and Z. Li, "SP-NAS: serial-to-parallel backbone search for object detection," in *CVPR*, 2020. **5, 6**
- [40] X. Dai, Y. Chen, B. Xiao, D. Chen, M. Liu, L. Yuan, and L. Zhang, "Dynamic head: Unifying object detection heads with attentions," in *CVPR*, 2021. **5, 6**
- [41] C. Wang, A. Bochkovskiy, and H. M. Liao, "Scaled-yolov4: Scaling cross stage partial network," *arXiv preprint arXiv:2011.08036*, 2020. **5, 6**
- [42] L. Shen, Z. Lin, and Q. Huang, "Relay backpropagation for effective learning of deep convolutional neural networks," in *ECCV*, 2016. **5**
- [43] C. Szegedy, W. Liu, Y. Jia, P. Sermanet, S. E. Reed, D. Anguelov, D. Erhan, V. Vanhoucke, and A. Rabinovich, "Going deeper with convolutions," in *CVPR*, 2015. **5**
- [44] C. Szegedy, V. Vanhoucke, S. Ioffe, J. Shlens, and Z. Wojna, "Rethinking the inception architecture for computer vision," in *CVPR*, 2016. **5**
- [45] Y. Cao, J. Xu, S. Lin, F. Wei, and H. Hu, "Global context networks," *TPAMI*, 2020. **6**
- [46] H. Zhang, C. Wu, Z. Zhang, Y. Zhu, Z. Zhang, H. Lin, Y. Sun, T. He, J. Mueller, R. Manmatha, M. Li, and A. J. Smola, "Resnest: Split-attention networks," *arXiv preprint arXiv:2004.08955*, 2020. **6**
- [47] Q. Xie, M. Luong, E. H. Hovy, and Q. V. Le, "Self-training with noisy student improves imagenet classification," in *CVPR*, 2020. **6**
- [48] G. Ghiasi, Y. Cui, A. Srinivas, R. Qian, T. Lin, E. D. Cubuk, Q. V. Le, and B. Zoph, "Simple copy-paste is a strong data augmentation method for instance segmentation," in *CVPR*, 2021. **6**
- [49] K. Chen, J. Wang, J. Pang, Y. Cao, Y. Xiong, X. Li, S. Sun, W. Feng, Z. Liu, J. Xu, Z. Zhang, D. Cheng, C. Zhu, T. Cheng, Q. Zhao, B. Li, X. Lu, R. Zhu, Y. Wu, J. Dai, J. Wang, J. Shi, W. Ouyang, C. C. Loy, and D. Lin, "MMDetection: Open mmlab detection toolbox and benchmark," *arXiv preprint arXiv:1906.07155*, 2019. **5**
- [50] Y. Jia, E. Shelhamer, J. Donahue, S. Karayev, J. Long, R. Girshick, S. Guadarrama, and T. Darrell, "Caffe: Convolutional architecture for fast feature embedding," in *ACM Multimedia*, 2014. **5**
- [51] K. Chen, J. Pang, J. Wang, Y. Xiong, X. Li, S. Sun, W. Feng, Z. Liu, J. Shi, W. Ouyang, C. C. Loy, and D. Lin, "Hybrid task cascade for instance segmentation," in *CVPR*, 2019. **5**
- [52] N. Bodla, B. Singh, R. Chellappa, and L. S. Davis, "Soft-NMS: improving object detection with one line of code," in *ICCV*, 2017. **5**

- [53] J. Dai, H. Qi, Y. Xiong, Y. Li, G. Zhang, H. Hu, and Y. Wei, "Deformable convolutional networks," in *ICCV*, 2017. 6
- [54] R. R. Selvaraju, M. Cogswell, A. Das, R. Vedantam, D. Parikh, and D. Batra, "Grad-cam: Visual explanations from deep networks via gradient-based localization," in *ICCV*, 2017. 9